Hybrid Renewable Energy System

Soham Joshi[1], Atharva Joshi[2], Jayendra Patil[3], Suyog Jare[4], Rojince Thomas[5]

Student, Dept. of Mechanical engineering, Vishwakarma institute of Technology, Pune.

---***---

ABSTRACT: *Power demand is on the rise for some time now and with climate change, depleting fossil fuels and increasing global warming the use of renewable energy sources, like solar, wind, geothermal, ocean etc., to meet the escalating power demand in a sustainable, cost-effective, and environment-friendly way is inevitable. However, the stability and availability of a single renewable source is not guaranteed.*

Combination of different sources making a hybrid renewable system are now being explored to overcome this problem. Wind turbine system combined with solar photovoltaic (PV), as a hybrid system, can play a significant role to overcome our future energy demands with a cost-effective energy system. This paper presents a hybrid system that uses both solar as well as wind energy to give a stable power supply all-round the year.

Key Words: *Solar, Wind energy, Hybrid Power, Renewable, Cooling, Vertical-Axis wind turbine etc.*

I. INTRODUCTION:

Better Health care, enhanced education, better transportation, superior communications systems, higher standard of living and economic stability are some of the major benefits of having usable electric power. However, many parts of the world still do not have a stable source of usable electricity with most non-electrified areas being in the developing nations.

Acknowledging this, many governments have undertaken huge electrification campaigns for rural regions. Renewable sources are being explored to overcome this demand. Wind turbine system combined with solar photovoltaic systems are becoming popular for standalone power generation applications. This is being seen as a good opportunity to reduce the dependence on fossil fuels and move towards a sustainable power supply. This system can be deployed in residential as well as commercial complexes as stand-alone power generation systems with great benefits even though, research and development are required to increase the efficiency of the solar panel and thereby the entire hybrid system.

In this paper a hybrid solar-wind power generation system is proposed for a residential complex with 60 apartments. The main objective of the Hybrid Renewable Power Generation System (HRPGS) is the production and utilization of the electrical energy coming from multiple sources, given that at least one of them is renewable (Gupta, 2008). Residential generating systems harnessing wind and solar energies are seen as a potential answer to individual energy concerns. The integration of renewable sources such as solar and wind are the is viewed as an answer for feeding the mini-grids and isolated loads.

II. DESIGN OF SOLAR ENERGY SYSTEM

The planet Earth has copious supply of sunlight. The amount of solar energy that the earth receives in one hour is over and above the planet's total energy requirements for a whole year. But the amount of solar energy that can used depends upon varies factors like, the time of day and the season of the year as well as the geographical location. Solar power systems, such as Photovoltaic (PV) systems, that convert the incident solar energy to electricity by using semiconductor devices like solar electric cells, are now being used to generate electrical power for households to counter their everyday energy necessity. Individual PV cells are arranged into panels of varying electricity-producing capacities. PV systems range from single PV cells for powering calculators to large power plants with hundreds of modules to generate large amount of electricity.

A. Determining Power Consumption Demands

Monthly power requirement for one house was recorded. Average units consumed were observed to be 137.66 and daily unit consumed were on an average 4.588.

Table 1: Monthly Power Requirements of one house

Month	Units Consumed
Jan	105
Feb	98
Mar	102
Apr	110
May	200
Jun	135
Jul	130
Aug	175
Sep	160
Oct	164
Nov	143
Dec	130
Avg	137.6666667
Daily	4.588888889

Power requirement for 60 houses was then calculated.

B. CALCULATING PANEL GENERATION FACTOR

Panel Generation Factor is required for calculating the size of the solar PV cells. It depends on various factors like he climate of the site location (depending upon global geographic location) etc.

Table 2: Panel Generation Factor

Avg Sol Rad	5.41
Loss cal for temp	0.85
Daylight loss	0.95
MPP	0.9
Dust loss	0.95
Ageing	0.9
Total power	0.62137125
PGF	3.36161846

The month wise Solar Radiation is shown in table given below:

Table 3 Month wise solar radiation

Month	Solar Radiation (MJ/day/m²)	Solar Radiation (kWh/day/m²)
January	17.29	4.802778162
February	20.58	5.716667124
March	23.11	6.419444958
April	24.49	6.802778322
May	25.18	6.994445004
June	19.32	5.366667096
July	16.1	4.47222258
August	15.68	4.355555904
September	18.73	5.202778194
October	19.25	5.34722265
November	17.64	4.900000392
December	16.45	4.56944481
Total	233.82	64.9500052
Average	19.485	5.412500433

Average solar radiation (kWh/day/m2) is found to be 5.41. Suppose the lowest month solar has a daily average of 5.412. That is equivalent to 5.41 hours of 1000 W/m2 sunlight every day. Loss calculation for temperature will be 15%, daylight not arresting the panel will be nearly 5%, MPP loss will be nearly about 10%, and dust will add up loss of 5%, ageing effect will have loss of 10% (J.Barad,2017). Hence total overall power was 0.621 of original panel rating. Panel generation factor came out to be 3.361.

C. CALCULATION OF PANEL REQUIREMENT

The total number of PV panels is obtained by dividing the total watt peak rating by rated output of watt peak of the PV modules available.

Table 4: Number of panels required.

P req	Watt	Number of panels	Price	Area m2
106476.5	40	2662	3825294	775.8399
106476.5	50	2130	3544320	725.8795
106476.5	60	1775	3216300	755.1738
106476.5	75	1420	3453440	746.849
106476.5	100	1065	3067200	738.5243
106476.5	160	666	4330332	660.4056
106476.5	320	333	2813850	556.1017
106476.5	330	323	2882775	632.5038
106476.5	340	314	3120218	526.22

D. CALCULATION FOR FIX TILT ANGLE

To calculate fix tilt angle, use below given methods to find the finest angle from the plane at which the module should be tilted:

Table 5: Latitude and fix tilt angle relation

Latitude	Fix Tilt Angle
Latitude<25	Latitude * 0.87
25<Latitude<50	(Latitude x 0.76) + 3.1°

E. Battery Selection

Average daily use is 4.60 kW of all appliances.

But we would not consider 4.6 kW as we will not run all appliances during a power cut, we will consider 310 kW which includes:

Table 6: Power Requirement

	Total required power kWh/day
For 60 houses	275.3333333
With F.S	357.9333333
`Total Wp of PV panel Cap needed	106.4764896

Table 7: Modeling of household applications

Appliances	Quantity	Rating	Load (W)
Fan	2	100	200
LED	3	15	45
Wi-Fi Router	1	25	25
L.E.D T.V	1	50	50
			310

F. PERFORMANCE ENHANCING OF PHOTOVOLTAIC PANELS BY WATER COOLING.

Sunlight incident on a solar panel generates heat and electricity. For a typical commercial PV module operating at its maximum power point, only 15 to 20%

of the incident sunlight is converted into electricity, while most of the rest is converted into heat. One of the main obstacles that face the operation of photovoltaic panels (PV) is overheating due to excessive solar radiation and high ambient temperatures. Overheating reduces the efficiency of the panels dramatically. The ideal P–V characteristics of a solar cell for a temperature variation between 0ₒC and 75ₒC are shown in Fig. The P–V characteristic is the relation between the electrical power output P of the solar cell and the output voltage, V, while the solar irradiance, E, and module temperature, T_m, are kept constant. If any of those two factors, namely T_m and E, are changed the whole characteristics change. The maximum power output from the solar cells decreases as the cell temperature increases, as can be seen in Fig. The temperature coefficient of the PV panels used is -0.5%/ₒC, which indicates that every 1ₒC of temperature rise corresponds to a drop in the efficiency by 0.5%. This indicates that heating of the PV panels can affect the output of the panels significantly.
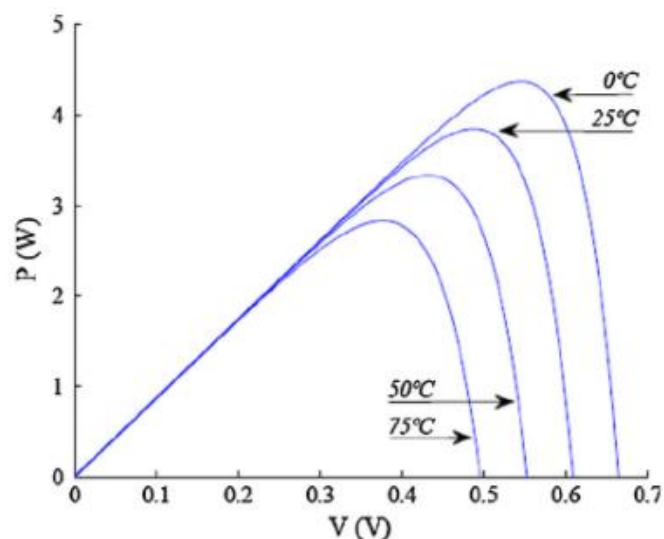
Fig 1*: P–V characteristics as a function of the module temperature Tm*

In order to avoid this overheating, cooling technique is the solution for it. Hybrid Photovoltaic/Thermal (PV/T) solar system is one of the most popular methods for cooling the photovoltaic panels nowadays. The hybrid system consists of a solar photovoltaic panel combined with a cooling system. The cooling agent, i.e., water or air, is circulated around the PV panels for cooling the solar cells, such that the warm water or air leaving the panels may be used for domestic applications such as domestic heating. It was also found that cooling the solar photovoltaic panel does not allow the solar cells surface temperature to rise above 46ₒC when exposed to solar radiation for a period of 4 hours.

A study shows, hybrid PV/T solar system was designed where water and air were both investigated in the

combined system as cooling agents. The water-based cooling system was found to increase the solar cells performance higher than the air-based cooling system. With water as cooling agent, it was found that cooling the solar photovoltaic panel it increases the solar cells output power by almost 50%.

Another study shows, a design of novel micro-heat pipe array for solar panels cooling. The cooling system consists of an evaporator section and a condenser section. The input heat from the sun vaporizes the liquid inside the evaporator section and then the vapor passes through the condenser section, and finally, the condenser section is cooled down using either air or water. Hence, the heat pipe can transfer the heat from solar panel to air or water depending on the system. Using air as a coolant was found to decrease the solar cells temperature by 4.7 ₒC and increases the solar panel efficiency by 2.6%, while using water as a coolant was found to decrease the solar cells temperature by 8 ₒC and the panel efficiency by 3%.

From the above study we can conclude that using water as a coolant is found to be more effective than using air.

The cooling rate model is developed to:
1. Minimize the energy input.
2. Minimize the amount of water.
3. Optimize time of cooling.

G.   MATHEMATICAL MODELING

i.   Heating Rate Model

- Cooling frequency is function of heating rate of panels.
- Objective was to find the module temperature as a function of time.

The module temperature is calculated using the following equation:

$$T_m = T_{amb} + \frac{(NOCT-20)\,E}{800}$$

Where T_m = Module Temperature, T_{amb} = Ambient Temperature, NOCT = Nominal Operating Cell Temperature, E = Solar Irradiance

The NOCT is a function of the ambient air temperature at the sunrise time T_{rise} as follows:

NOCT = 20ₒ + T_{rise}

The rate of heating of the PV panel, $\frac{dT_m}{dt}$, is dependent on the following: (i) the ambient temperature, (ii) the irradiance, and (iii) the NOCT. The NOCT has a constant value, while the irradiance and the ambient temperature are functions of time. Therefore, the module temperature will be function of time between sunrise and sunset.

In general, this heating rate comes out to be 6°C/hr. or 0.1°C/min. (These are the values observed experimentally and so used directly)

ii.   Cooling Rate Model

- Cooling rate is found by energy balance.
- Critical from the point of energy consumption

The cooling time t is determined from the following energy balance:

$Q_{gained\ by\ cooling\ water}$ = $Q_{dissipated\ from\ PV\ panels}$

$\dot{m}_w \times t \times c_w \times \Delta T_w = m_g \times c_g \times \Delta T_g$

$t = \dfrac{m_g \times c_g \times \Delta T_g}{\dot{m}_w \times c_w \times \Delta T_w}$

Where $\dot{m}_w$ = mass flow rate of water,
m_g = mass of glass,
c_w = specific heat capacity of water,
c_g = heat capacity of glass,
ΔT_w = water temperature rise ,
ΔT_g = glass temperature changes due to water cooling.

The mass flow rate of water $\dot{m}_w$ is calculated from the equation: $\dot{m}_w = \rho_w \dot{V}$, where ρ_w is the water density and $\dot{V}$ is the volume flow rate. The mass of glass m_g is calculated from the equation: $m_g = \rho_g A_g x_g$, where ρ_g is the density of tempered glass, A_g is the surface area of the PV panel, and the x_g is the thickness of the glass covering the PV panel. The heat capacity of water, c_w, and the heat capacity of glass, c_g, are assumed to be constant since the variation in the water and the PV panel temperature is not large.
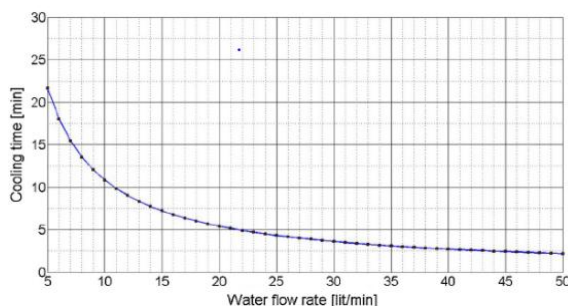

Fig 2: Cooling time t versus volume flow rate

Temperature of solar panel before cooling = 45° C

Temperature of solar panel after cooling = 35° C

Temperature of water at inlet = 25° C

Temperature of water at outlet = 35° C (assumed that water leaves at some temperature)
$$\Delta T_g = \Delta T_w = 10°\ C$$

III.   ANALYSIS AND OPTIMIZATION OF VAWT

Wind is plentiful source of clean energy. To harness electricity from wind energy, wind turbines use blades to collect the wind's kinetic energy. Wind flows over the blades creating lift, which causes the blades to turn. The blades are connected to a drive shaft that turns an electric generator, which produces electricity. Wind turbines can be classified in a first approximation according to its rotor axis orientation and the type of aerodynamic forces used to take energy from wind. There are several other features like power rating, dimensions, number of blades, power control, etc. that are discussed further along the design process and can also be used to classify the turbines in more specific categories.

A.   ROTOR AXIS ORIENTATION

The major classification of wind turbines is related to the rotating axis position in respect to the wind; care should be taken to avoid confusion with the plane of rotation:

i.   Horizontal Axis Wind Turbines (HAWT):

The rotational axis of this turbine must be oriented parallel to the wind in order to produce power. Numerous sources claim a major efficiency per same swept area and the majority of wind turbines are of this type.

ii.   Vertical Axis Wind Turbines (VAWT):

The rotational axis is perpendicular to the wind direction or the mounting surface. The main advantage is that the generator is on ground level, so they are more accessible, and they do not need a yaw system. Because of its proximity to ground, wind speeds available are lower.

B.   DESIGN OF 600W HELICAL BLADE VERTICAL AXIS WIND TURBINE

In the case of a horizontal-axis wind turbine, a large number of devices are required, such as a yawing device and a pitching device. While the generation efficiency is relatively high, the blade shape is complicated. There is also a disadvantage in that the wind direction is limited. In the case of a vertical-axis wind turbine, the structure is simple, and it is advantageous for installation in a city center because there is no restriction of the wind direction.

Typical blade types of vertical-axis wind turbines are Darrieus, gyro-mill, Savonius, and helical blades. The helical type is advantageous in that the fluctuation range

of the output is smaller than that of the conventional Darrieus or gyro-mill blades, and the self-starting performance is better. It also has less mechanical load and less noise than a Savonius rotor, which is a drag-type rotor.

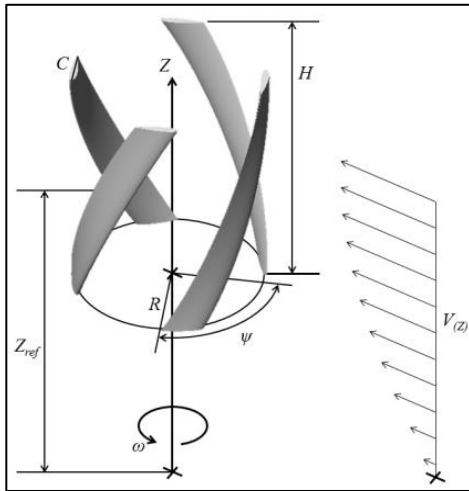$$P = \frac{1}{2}\rho A_\omega V^3 \qquad (1)$$

Fig 3: Basic design parameters of the vertical wind turbine

Equation (2) is the mechanical power output generated by the rotation of the wind turbine rotor.

$$P = T\omega \qquad (2)$$

The ratio of the power converted from the rotor power to the wind power flowing is called the power coefficient, which is a concept of aerodynamic energy conversion efficiency. Theoretically, the maximum value of the power coefficient is 0.593 in a horizontal axis wind turbine, which is known as the Betz limit. The Betz limit is derived from actuator disk momentum theory and is the theoretical maximum assuming that the flow is steady-state, inviscid, and irrotational. The Darrieus turbine is a typical lift-type vertical-axis wind turbine and has a maximum power coefficient of about 0.4 at a tip speed ratio of 5.

Equation (3) shows the power output (P) of the wind turbine considering the power coefficient (C_P) and power transmission efficiency (η). A_ω is the rotor swept area (see Equation (5))

$$P = \frac{1}{2}\rho A_\omega V^3 \eta C_p \qquad (3)$$

The tip speed ratio (λ) is closely related to the power coefficient. The tip speed ratio is defined as the ratio of the blade tip speed and the wind speed at which the blade tip moves with rotation, as shown in Equation (4).

$$\lambda = \frac{R\omega}{V} \qquad (4)$$

All wind turbine rotors have an optimum tip speed ratio with maximum power. The optimal ratio is related to the change of the incoming wind speed. The rotor swept area (A_ω) is determined by the radius and height of the wind turbine.

$$A_\omega = 2RH \qquad (5)$$

The wind-swept area should consider the height of the rotor (H) and the aspect ratio with respect to the radius (R). The longer the rotor radius, the higher the generated torque, but the longer the strut length, the lower the structural stability. However, when the rotor height is greater, the generated torque is lower, and the rotational speed of the rotor should be increased to obtain the same power output. The aspect ratio (AR) can be expressed as

$$AR = \frac{H}{2R} \rightarrow H = AR \times 2R \qquad (6)$$

Solidity (σ) is an important variable that determines the performance of wind turbines. Solidity is defined as the ratio of the total projected area (NC) of the rotor blade to the rotational area of the wind turbine rotor. The projected area is the projection in the vertical section of the rotating shaft and can be expressed as

$$\Sigma = \frac{NC}{2\pi R} \qquad (7)$$

The blade chord length (C) can be calculated using the solidity. The chord length is the length of the airfoil and is an important design variable because the generated torque changes according to the chord length.

Urban wind power generators should operate at low speed with low noise. A Savonius wind turbine can rotate with a tip speed ratio of less than 1, but the vibration and noise are severe due to the characteristics of a drag-type rotor. Among the lift type vertical-axis wind turbines, helical-blade wind turbines have a narrower range of output fluctuation compared to Darrieus and gyro-mill wind turbines, and their efficiency is higher due to the larger wind-swept area.

The purpose of this study is to design a low-speed vertical-axis wind turbine blade with a tip speed ratio of 1.1 at a rated wind speed of 10 m/s. The design of wind turbine with the designer-defined Class S after modifying Class 1 identified in IEC 61400-2; Figure shows a picture of the basic parameters of the small wind turbine system. The selected rated wind speed was 10 m/s, which is lower than the rated wind speed corresponding to Class 1. The height of the rotor hub is 8 m. Wind shear is

considered, and the velocity profile (V(Z)) is shown in Equation (8).

$$V(Z) = V_{ref} (Z/Z_{ref})^a \qquad (8)$$
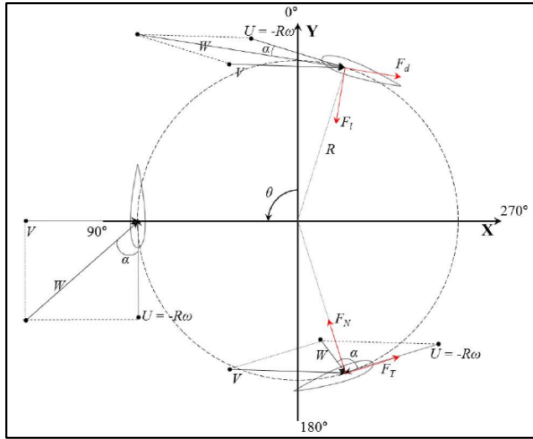
Fig 4: *Force and velocities acting on the vertical wind turbine for various azimuth angles.*

The wind shear power index (a) can be varied according to the surface roughness of the terrain. In this study, 0.23 was selected for the condition of a forest or a small number of buildings. Table summarizes the design parameters applied in this study. The maximum wind speed, turbulence intensity, and dimensionless slope are the same as Class 1. The target output is 600 W, and the air density is 1.225 kg/m³, as specified in IEC 61400-2. The power transmission efficiency was assumed to be 95%, and the average power coefficient turbine was set as 0.15. The design output, air density, design wind speed, and efficiency are defined in Equation (3).

Equation (9) is used for calculating the radius of the wind turbine rotor through the relationship between the wind-swept area and the aspect ratio. A radius of 0.55 m and height of 1.43 m were thus chosen.

$$R = \sqrt{\frac{A_\omega}{4 \times AR}} \qquad (9)$$

A tip speed ratio of 1.1 was chosen. In the case of a Darrieus-type wind turbine, the maximum power coefficient can be achieved at tip speed ratios between 4 and 6. At the designed wind speed of 10 m/s with a rotor radius of 0.45 m, the rotational speed is between 230 and 500 rpm, which is inadequate for use in a city center. A rotational speed of 230 rpm was derived by applying the radius, design wind speed, and tip speed ratio in Equation (4). The number of blades was chosen as 3, and the solidity was set as 0.3, which was substituted into Equation (7) to determine the chord length of 0.25 m.

In this study, the aerodynamic power of the wind turbine rotor was investigated by applying a NACA 0018 airfoil

and a mathematical model using the lift and drag forces of the airfoil according to the angle of attack. Unlike the blade of a horizontal-axis wind turbine, which has a fixed angle of attack, the angle of attack varies for a vertical-axis wind turbine depending on the rotation angle of the rotor.

Table 8: Blade specifications

Item	Description
Rotor type	Helical
Rated power output	600 W
Rated wind speed	10 m/s
Transmission efficiency	0.95
Swept area	1.37 m²
Aspect ratio	1.64
Rotor radius	0.45 m
Rotor height	1.5 m
Rotational speed	230 rpm
Solidity	0.3
Chord length	0.25 m
Number of blades	3
Airfoil	NACA0018

Figure presents the tip velocity vector and the lift, and the drag vectors generated by the rotation of the turbine blade. The angle of attack changes with the blade tip velocity vector and the influx wind velocity vector. The vector sum (W) of the tip velocity vector and incoming wind velocity vector (V) is calculated by Equation (10). The maximum value occurs at θ = 0º, and the minimum value occurs at θ = 180

$$W = \sqrt{V^2[(\lambda - \sin^2\theta)^2 + \cos^2\theta]}$$
$$= V\sqrt{1 + 2\lambda\cos\theta + \lambda^2} \qquad (10)$$

The angle of attack (α) is the angle between the vector sum and the direction of the chord length. As the vector sum changes, the angle of attack has a positive value in the upstream region of the rotor and a negative value in the downstream region. The angle of attack can be expressed as Equation (11)

$$\alpha = \tan^{-1}\left(\frac{\sin\theta}{\cos\theta + \lambda}\right) \qquad (11)$$

As shown in the equation, the dominant variable that affects the angle of attack is the tip speed ratio. Figure shows the angle of attack as the blade rotates according to the tip speed ratio. The larger the tip speed ratio, the smaller the range of the angle of attack the airfoil receives during rotation. The larger the blade tip velocity vector is, the larger the tip speed ratio is. This occurs because the vector sum direction approaches the direction of the blade's forward velocity vector, and the angle of attack becomes smaller. The range of the angle

of attack of the airfoil is about $\pm 66.5^{o}$ in one rotation of the rotor.
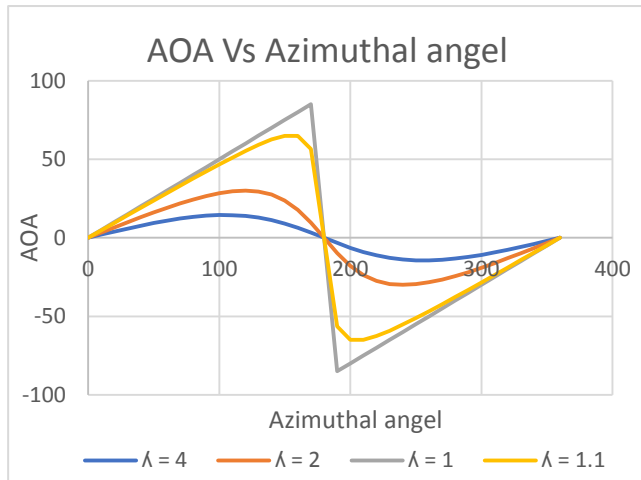

Fig 5: Angle of attack variation in a blade revolution for different tip speed ratios.

Table shows the angle of attack at rotor rotation angles of 0° to 180° when the tip speed ratio is 1.1.

Table 9: Angle of attack in blade revolution (λ=1.1)

Azimuth Angle [^{o}]	AOA [^{o}]
0	0.000
10	4.789
20	9.575
30	14.354
40	19.122
50	23.875
60	28.607
70	33.311
80	37.976
90	42.589
100	47.127
110	51.558
120	55.929
130	59.840
140	63.400
150	66.069
160	66.568
170	59.298
180	0.000

The lift and drag coefficients (C_L, C_D) of the NACA 0018 in Table are defined in Equations (12) and (13), respectively.

$$C_L = \frac{F_L}{\frac{1}{2}\rho c H W^2} \qquad (12)$$

$$C_D = \frac{F_D}{\frac{1}{2}\rho c H W^2} \qquad (13)$$

Table summarizes the boundary conditions applied to 2D CFD analysis. The inlet was set to 9 m/s, which is the design wind speed, and the outlet conditions were pressure boundary conditions. The area around the rotor is divided into separate areas, and the rotor area is given a rotation condition and the rest area is given a stop condition. The rotation speed was 170 rpm and the surface of the blade was subjected to the adhesive condition. The analysis was carried out by transient analysis and the time interval was given a time corresponding to the rotor rotation angle of 1°. For the inlet fluid, air with a density of 1.225 kg/m³ at 1 atm and 25 ^{o}C specified in IEC 61400-2 was applied and the turbulence intensity was 18%. The URANS analysis was carried out as a transient analysis. The time interval was about 9.8×10^{-4}s corresponding to 1° of rotor rotation. The turbulence model adopted the same SST turbulence model.

Table 10: Boundary conditions for 2D CFD analysis

Item	Description
Inlet	10 m/s
Outlet	Atmospheric pressure (Opening condition)
Side	Free-slip condition
Blade surface	No-slip condition
Rotational speed	230 rpm
Rotational direction	Counter-clockwise

Figure shows the lift and drag coefficients of the airfoil at each angle of attack obtained from the two-dimensional steady-state CFD analysis.
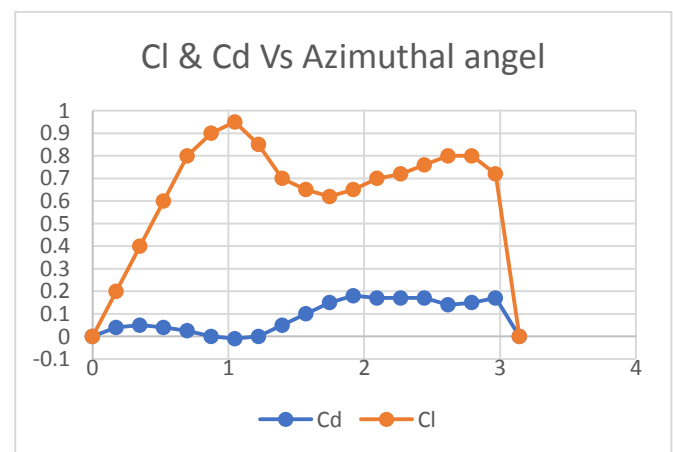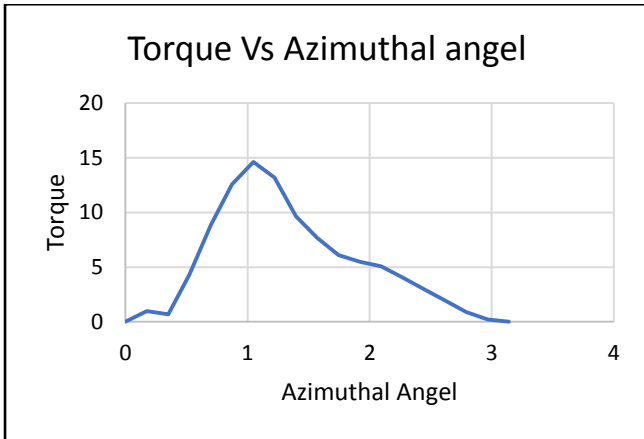

Fig 6: Graph of Lift and drag coefficient variation in a blade azimuth angle from 0o to 180 (NACA0018) calculated by 2D CFD simulation

Fig 7: Graph of Torque versus Azimuthal angle
(Angle of rotation)

The normal coefficient (C_N) and the tangential coefficient (C_T) are generated from the blade by using the lift coefficient and the drag coefficient and calculated using Equations (14) and (15).

$$C_N = C_L \cos \alpha + C_D \sin \alpha \qquad (14)$$
$$C_T = C_L \sin \alpha - C_D \cos \alpha \qquad (15)$$

The normal force (F_N) and tangential force (F_T) of the blade can be calculated through the normal and tangential coefficients using Equations (16) and (17).

$$F_N(\theta) = \frac{1}{2}\rho cHW^2 C_N \qquad (16)$$
$$F_T(\theta) = \frac{1}{2}\rho cHW^2 C_T \qquad (17)$$

The power output can finally be calculated using the blade torque (Equation (18)) and the angular velocity using the tangential force:

$$T(\theta) = \frac{1}{2}\rho cHW^2 C_T R \qquad (18)$$

The instantaneous and average power output of the designed rotor are given by Equations (19) and (20)

$$P(\theta) = T(\theta) \times \omega \qquad (19)$$

$$P(\theta) = \frac{N}{2}\pi\int_0^\pi P(\theta)d\theta \qquad (20)$$

IV. CFD

The CFD simulation was carried out in OpenFoam. It was transient simulation

Table 11: System Parameters

Parameter	Description
Flow domain	Rectangle (4mx2m)
Interface	Sliding
Grid/type	Structured/quad
Elements	251,723
Fluid	Air

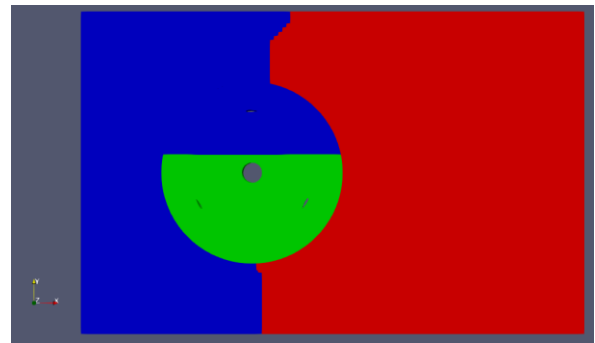|	
Turbulence model	k-ω SST
Inlet	Velocity inlet
Outlet	Pressure outlet
Shaft	No-slip wall
Blades	No-slip wall

A. MESH

The meshing was done using snappyhexMesh and also a rotating Mesh was defined for the rotating blades.
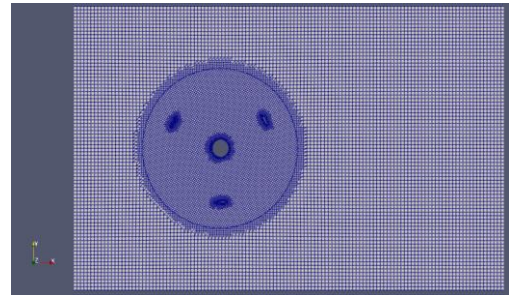
Fig 8: Mesh

B. DIVISION OF DOMAIN

The Domain was divided into 3 parts using *decomposePar* command so that the solution can be run parallelly.

Fig 9: Division of Domain

C. RESULTS:

The results of the simulation are shown below. *Paraview* was used for doing the post processing part. The velocity and pressure contours were visualized.
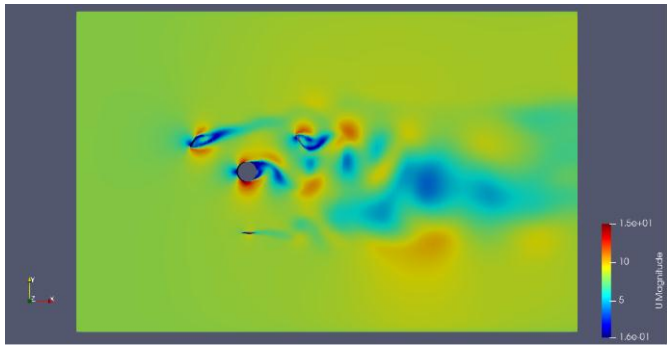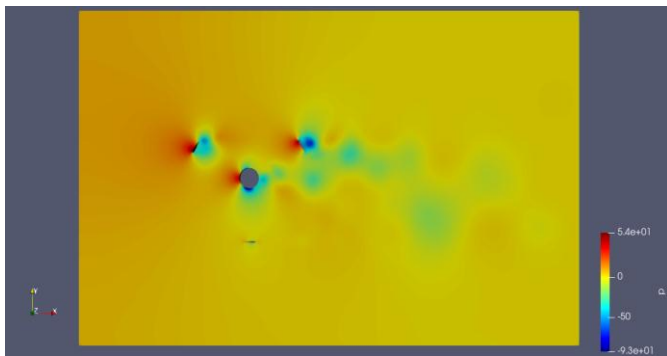
Fig 10: Pressure Contour
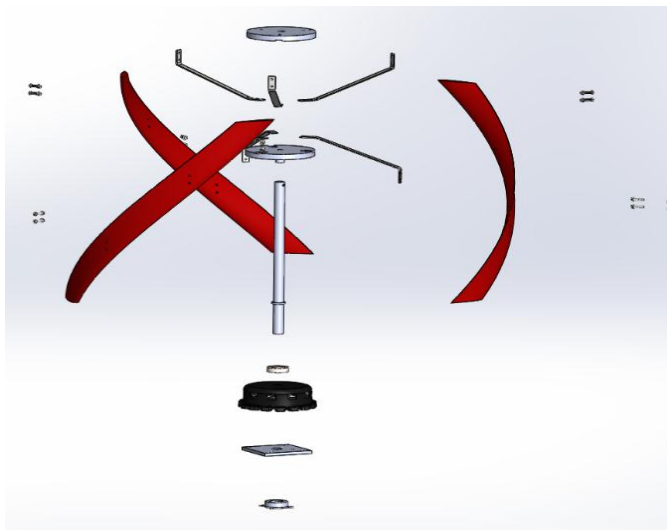

Fig 11: Velocity Contour

CAD MODELLING

Fig 12: Exploded View
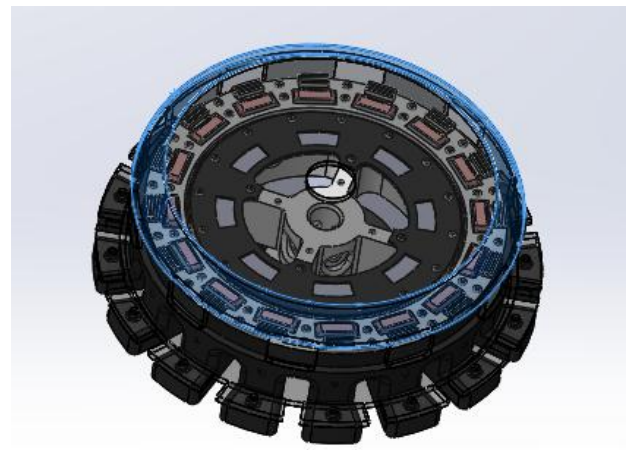

Fig 1: Rendered Model

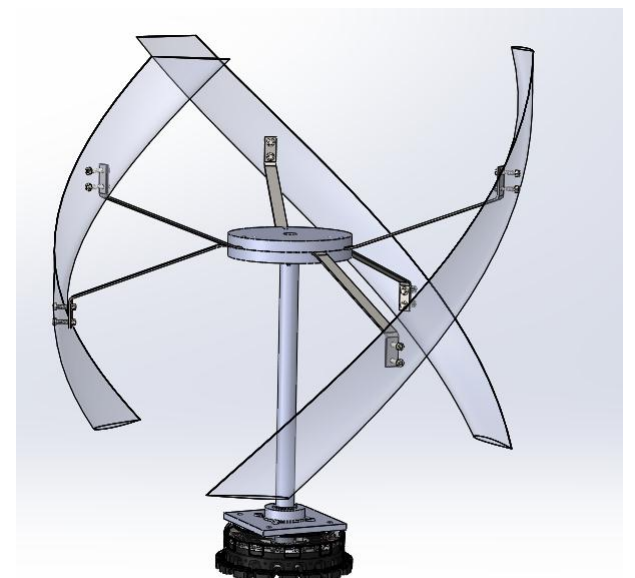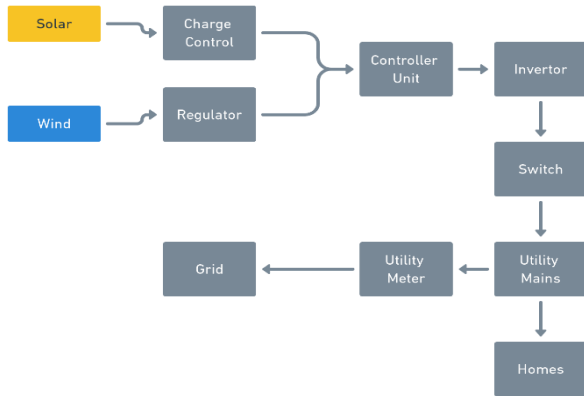**Fig 2**: Alternator

Fig 3

V. INTEGRATION OF THE SYSTEMS

The solar wind power generation system is designed as shown below:



Fig 4 : Flow Chart

The control unit plays two roles.

- It controls the operation of the inverter. That is if it senses solar energy, it automatically switches off the inverter and allows only charging of battery. This also means that the control unit switches OFF the inverter during the day and switches ON at night.

- It controls the modulation of the inverter through the feedback loop by adjusting the modulation current.

When solar radiation falls on the solar panel, DC electricity flows. This electricity flows through the charge controller which regulates the DC energy for efficient charging. Similarly, when wind blows over the blades of the turbine, it turns the DC generator. The electricity generated is used for battery charging. The powers from the solar panel and the wind turbine add up when the two sources are at reasonable potentials. When the wind speed is below the cut-in point, and in a sunny day, solar energy takes over the charging. If on the other hand the wind speed is reasonably high and no solar radiation, especially at night, the wind turbine takes over.

VI.   SIMULINK MODEL

We modelled the solar and wind turbine generation together with energy consumption model to understand the renewability of the hybrid system employed. We have taken 200 solar panels and 20 wind turbines in the below model. Which can be varied easily as it used as constant block. We have used the 24hrs of hourly data in the model to understand the net generation to consumption as well. As the system is going to work on net billing i.e., supply is provided to grid when excess generation takes place and supply is taken from grid when requirements exceed the generation.
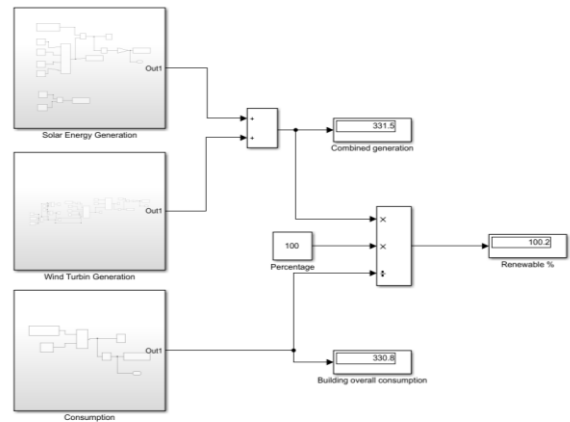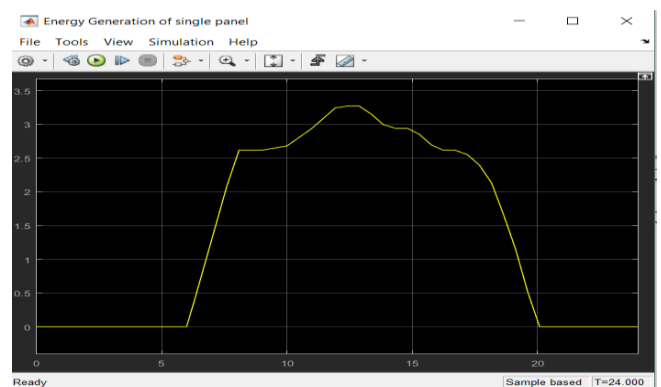

Fig 5: Complete Integrations of wind & solar
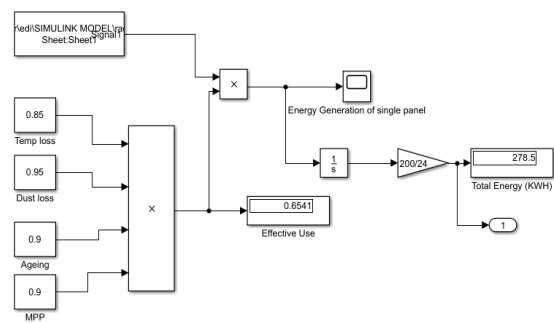
Fig 6: Solar Energy generation model.

Solar model consists of spreadsheet with varying the generation as with time (at night 7pm to 7 am) generation is considered zero. Also, the factors like ageing, temp loss, and dust loss are calculated.
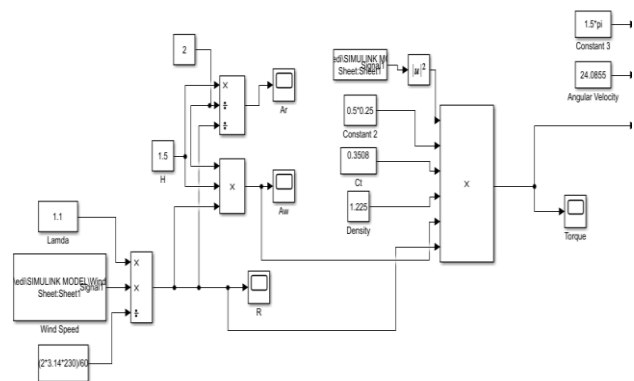

Fig 7: Daily Generation for single panel
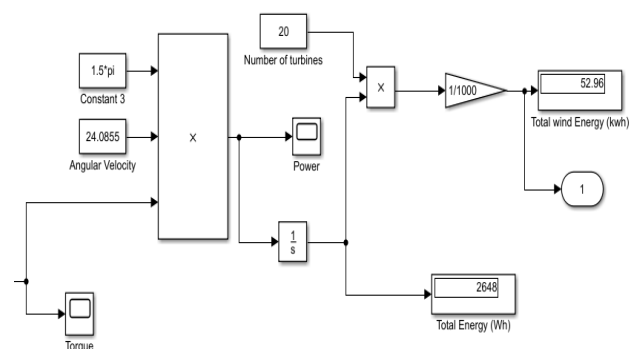
Figure 8: Wind energy model
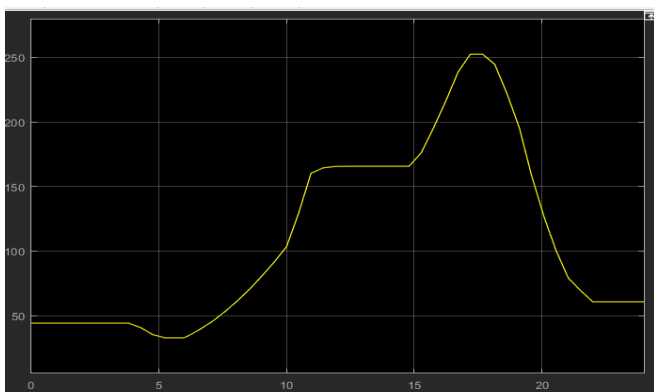

Fig 9: Wind energy model II

Fig 10: Daily wind turbine generation model

Similar wind turbine model gives us the energy generation in a day with varying wind speed and this is taken from meteorology department website for a day on hourly basis.

VII. CONCLUSION.

The paper presents a design of a hybrid renewable energy setup with the help of solar and wind energy. In design aspect the focus was on improving the efficiency of solar panel as it lies in range of 15%. 33% increase in efficiency was observed when the solar panels were provided cooling. They operate at 20% now. In the wind turbine focus was on enhancing the performance by

shape optimization, number of blades and CFD was done for analysis.

As there can be space constraint so 100% renewable maybe difficult for some regions, a percentage of renewable source can be used. A cost model was also developed keeping in mind the cost and space and make the system affordable on the basis of percentage of renewable source used.

The SIMULINK model considers number of solar panel and wind turbines so we can change them based on our space and cost constraint and Complete Integrations of wind & solar model (Fig. 17) will give us renewability percentage and thus help us understand Overall CO_2 emission reduction. This is calculated in table below as well. This table showcases tree equivalent for one day consumption and if expanded shows huge role in explaining worth of our work.

CO2 emission & Number of Trees Equivalent	% Renewable	KWH	Kg of CO2	Trees Equivalent
	100	1	0.429	0.05753
	100	357.93	153.55	2,669.10
	70	250.55	107.49	1,868.37
	50	178.97	76.78	1,334.55

Fig 11: Percentage Renewable and Trees equivalent.

VIII. REFERENCES

1) Jayesh S. Barad; Mahesh S. Chauhan; Dharmesh S. Barad, Prof. Hitesh Parmar. Calculation methodology and development of solar power generating system for household appliances. 2017, 4, 2456-4184.

2) K.A. Moharram; M.S. Abd-Elhady; H.A. Kandil; H. El-Sherif. Enhancing the performance of photovoltaic panels by water cooling. 2013, 4, 869-877.

3) Roshan Bhagat and Dr. Samir Deshmukh, "THERMAL MANAGEMENT OF SOLAR PHOTOVOLTAIC PANEL (PV) FOR PERFORMANCE ENHANCEMENT: A REVIEW", *IEJRD - International Multidisciplinary Journal*, vol. 5, no. 1, p. 9, Jan. 2020.

4) Yogesh S Bijjargi, Kale S.S and Shaikh K.A. Cooling Techniques for Photovoltaic Module For Improving Its Conversion Efficiency: A Review. 2016 0976-6340

5) Dr. E.D. Francis, B. Raghu, D.Vera Narayana. Cooling Techniques For Photovoltaic Module For Improving Its Conversion efficiency: A Review. 2016, 2278-7461

6) Oumaima Bendra. Optimizing Solar Cells Efficiency by Cooling Techniques. Capstone Design. 2017

7) J Castillo, Small-Scale Vertical Axis Wind Turbine Design, Bachelor's Thesis, Tampere University of Applied Sciences, December 2011.

8) Han, Dowon & Heo, Young & Choi, Nak & Nam, Sang & Choi, Kyoung & Kim, Kyung. (2018). Design, Fabrication, and Performance Test of a 100-W Helical-Blade Vertical-Axis Wind Turbine at Low Tip-Speed Ratio. Energies. 11. 1517. 10.3390/en11061517.

9) Magdi Ragheb and Adam M. Ragheb, Wind Turbines theory - The Betz Equation and Optimal Rotor Tip Speed Ratio. 2011,10.5772/21398

10) Pellegri, Adriano. The Complementary Betz's Theory. 2019

11) Tao Wei, WenXuan Gou, Chao Fu, YongFeng Yang, Transient Analysis of Speed-Varying Rotor with Uncertainty Based on Interval Approaches, *Discrete Dynamics in Nature and Society*, vol. 2018, Article ID 5904724.

12) Chandragupta Mauryan.K.S, Nivethitha.T, Yazhini.B, Preethi.B. Study on Integration of Wind and Solar Energy to Power Grid. 2014, 2248-9622.

13) Eriksson, S.; Bernhoff, H.; Leijon, M. Evaluation of different turbine concepts for wind power. Renew. Sus. Energy Rev. 2008, 12, 1419–1434.

14) Medugu, D. W. & Michael, E. Integrated Solar – Wind Hybrid Power Generating System for Residential Application. 2014, 2249-4596.

IX. BIOGRAPHIES

Soham Joshi has completed bachelor's in Mechanical Engineering from the Vishwakarma Institute of Technology, Pune. He is interested in Renewable Energy, Quality Assurance and Lean Methodology.

Atharva Joshi has completed bachelor's in Mechanical Engineering from the Vishwakarma Institute of Technology, Pune. He has worked in Formula Student competitions and holds interest in Research and Sustainable development, operations and six Sigma.

Jayendra Patil has completed bachelor's in Mechanical Engineering student from the Vishwakarma Institute of Technology, Pune. He has worked in SAE Baja competitions and is interested in Automobile, automation and additive manufacturing.

Suyog Jare has completed bachelor's in Mechanical Engineering student from the Vishwakarma Institute of Technology, Pune. He has worked in SAE Baja competitions and is interested in Automobiles, Supply chain analytics and Operational research.

Rojince Thomas has completed his B.Tech. degree in Mechanical Engineering from Vishwakarma Institute of Technology, Pune, India. He has a keen interest in Supply Chain Management, Quality Control, and Lean Methodology. Rojince is also curious about painting and music.